Acta Cryst. (1958). **11**, 696

Structural, Dielectric and Optical Properties of Ferroelectric Lead Metaniobate

BY M. H. FRANCOMBE AND B. LEWIS

Research Laboratories of The General Electric Company Limited, Wembley, England

(*Received* 17 *March* 1958)

X-ray structural, electrical and optical studies have been made of both single-crystal and ceramic specimens of ferroelectric $PbNb_2O_6$. High-temperature X-ray powder data show that above 560 °C., the Curie temperature, the structure changes from orthorhombic to tetragonal, and that the paraelectric structure is closely related to that of certain tetragonal alkali tungsten bronzes.

Plate-like single crystals of $PbNb_2O_6$ show a domain structure indicating ferroelectric polarization along the [010] axis. Along this axis and along [100], but not along [001], there is a sharp permittivity maximum at the Curie temperature.

Structural and electrical data for solid solutions of the type $PbO.xNb_2O_5$ with $1 \leq x \leq 3$ show that as x is increased the orthorhombic structure typical of pure $PbNb_2O_6$ changes to a tetragonal tungsten–bronze symmetry like that possessed by $K_{0.57}WO_3$ or $Na_{0.28}WO_3$. When $x > 1$ the structures are not ferroelectric. Replacement of Nb by Ta in the solid solutions $PbNb_2O_6$–$PbTa_2O_6$ is found to weaken the orthorhombic distortion characteristic of pure $PbNb_2O_6$, and results in a degeneration of ferroelectric properties.

A simple model is proposed to account for the ferroelectric properties of the $PbNb_2O_6$ structure and for the disappearance of ferroelectricity in the system $PbO.xNb_2O_5$ as x exceeds 1.

1. Introduction

Ferroelectricity is known to occur in several niobate structures, notably the perovskite-type $KNbO_3$ (Shirane, Danner, Pavlovic & Pepinsky, 1954) and the pyrochlore-type $Cd_2Nb_2O_7$ (Jona, Shirane & Pepinsky, 1955). The pseudo-ilmenite-type $LiNbO_3$ (Matthias & Remeika, 1949) has also been reported as ferroelectric. These compounds satisfy the criteria proposed by Matthias (1951) in that the structures contain a highly polarizable ion possessing a noble gas electronic configuration, in this case Nb^{5+}, and that this ion is enclosed in an oxygen octahedron.

Ferroelectricity in a niobate of another structural type, lead metaniobate, $PbNb_2O_6$, was discovered by Goodman (1953), who has described the electrical and structural properties of ceramic preparations and structural and optical properties of small single crystals. The structure is orthorhombic and is unique in the class of ferroelectrics satisfying Matthias's first criterion in that it is not pseudo-cubic. Further X-ray work (Francombe, 1956) has revealed that $PbNb_2O_6$ has two structural forms: (*a*) a non-ferroelectric form, stable to about 1200 °C., with a rhombohedral structure which may be described as a degenerated perovskite-type; (*b*) the ferroelectric allotrope, formed at temperatures above 1250 °C., which has an orthorhombic structure.

On cooling through the Curie temperature the pseudo-cubic ferroelectrics undergo a structure transition from a higher-symmetry paraelectric form by the creation of a polar moment and the simultaneous extension of the unit cell along the polar axis. A crystal is not normally uniformly polarized but contains domains with polarization of differing orientation. Structural and optical studies extending above the Curie temperature are necessary to determine the relation of the polar axis to the structure, and such measurements have now been carried out with single crystals of $PbNb_2O_6$.

As a further step in elucidating the structure it is desirable to break down the large unit cell into smaller structural groups and to determine the linkages between these groups. To this end studies have been made of compounds in the system $PbO.xNb_2O_5$, with $1 \leq x \leq 3$, and also of the solid solutions $PbNb_2O_6$–$PbTa_2O_6$.

2. Preparation

Ceramic and single-crystal specimens of $PbO.xNb_2O_5$ with $1 \leq x \leq 3$, and of solid solutions $PbNb_2O_6$–$PbTa_2O_6$, were prepared by a two-stage method. In the first stage a mixture of molar quantities of the appropriate oxides was fired in air at 1000 °C. X-ray examination of $PbNb_2O_6$ at this stage showed the rhombohedral form together with a trace of the orthorhombic form. After crushing and milling the powder was then used as material for the second stage of preparation.

Ceramic specimens were fired in air, as pressed discs, in the range 1250 to 1280 °C. With $PbNb_2O_6$ pale blueish-green specimens with the orthorhombic ferroelectric structure were usually obtained, with densities between 5·8 and 6·0 g.cm.$^{-3}$. The ideal density is 6·7 g.cm.$^{-3}$. On a number of occasions the rhombohedral form of $PbNb_2O_6$ was produced. This form is orange in colour and is thus easily distinguished. It appears to be the stable form up to about 1200 °C., but it was also obtained several times in specimens fired at 1250 °C. or even 1280 °C. Sometimes a few large orange crystallites were found embedded in a fine-grained orthorhombic ceramic matrix, but on other occasions most of the disc was rhombohedral although the surface was usually orthorhombic. In these cases the density was about 5·5 or less, the crystallite size was very large, and the ceramic was extremely brittle. It seems that although the rhombohedral form may be only metastable at 1250 °C. it does not always transform into the orthorhombic form at that temperature, particularly if it is present as large crystallites.

Small crystals of orthorhombic $PbNb_2O_6$ and of the compositions $PbO.x(Nb_2O_5)$, intended for X-ray and optical examination and for some electrical measurements, were grown from the melt in a platinum boat or crucible using firing temperatures of about 1330 to 1350 °C. For pure $PbNb_2O_6$ the crystals were pale yellow or yellow-green in colour, while with $x > 1$ they were green. Slow cooling in all cases yielded a crystalline mass from which crystals with dimensions up to 1 mm. could be separated. With $PbNb_2O_6$, plate-like crystals were occasionally obtained with the large faces up to about 3 mm. across.

3. Structure and polymorphic transitions in ferroelectric $PbNb_2O_6$

3·1. *Room-temperature structure*

In an earlier single crystal study of $PbNb_2O_6$ (Francombe, 1956) the orthorhombic unit-cell dimensions, calculated from single-crystal rotation photographs were reported as

$$a_0 = 17{\cdot}51, \quad b_0 = 17{\cdot}81, \quad c_0 = 7{\cdot}73 \text{ Å} .$$

Using these values it was found possible to index several of the complex diffraction-line groups in X-ray photographs taken of powdered single-crystal material. Orthorhombic unit-cell dimensions were calculated from diffraction lines with *hkl* indices (350, 530), (280, 820), (152, 512), and (004). The accuracy is estimated at about ±0·01 Å for the a_0 and b_0 parameters and ±0·005 Å for the c_0 parameter. The values obtained were

$$a_0 = 17{\cdot}65, \quad b_0 = 17{\cdot}91, \quad c_0 = 7{\cdot}736 \text{ Å} .$$

These are in good agreement with values given recently by Roth (1957):

$$a_0 = 17{\cdot}63, \quad b_0 = 17{\cdot}93, \quad c_0 = 3{\cdot}868 \text{ Å} .$$

Roth's value for c_0 is consistent with the powder data taken alone, but single-crystal rotation photographs for the [001] axis show quite clearly weak first and third order layer lines for a c_0 spacing of 7·736 Å. The discrepancies between these results and those derived previously from single-crystal data may be attributed to two causes. Difficulty was experienced in choosing single-domain crystals free from twinning, and thus high-order layer-line spots on single-crystal rotation photographs invariably showed splitting effects due to diffraction contributions from two types of domain (see Section 5 on optical studies). Errors also arose, in the single-crystal determinations, from high absorption in the crystals and from geometrical distortion due to the irregular plate-like habits.

3·2. *High-temperature X-ray study*

X-ray powder photographs were taken over the temperature range 20 to 800 °C. for powdered single-crystal material, using a Unicam. 19 cm. high-temperature camera and copper $K\alpha$ radiation.

The variation of lattice parameters with change in temperature is shown graphically in Fig. 1. As the temperature is raised from 20 °C. to about 560 °C. the a_0 unit-cell dimension increases in value and the b_0 dimension decreases slightly until both approach a common value. Over the same temperature range the c_0 dimension increases linearly. On passing through the transition temperature to about 575 °C. a marked, discontinuous change occurs in the cell dimensions; a_0 and b_0 both suddenly decrease to the same value, while c_0 increases sharply by approximately 0·04 Å. The overall effect on the unit-cell volume is a decrease of about 0·33%.

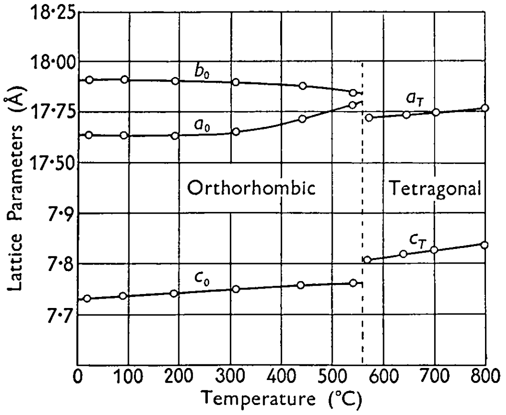

Fig. 1. Lattice parameters of $PbNb_2O_6$.

The paraelectric structure at 600 °C. is similar to that described by Roth (1957) for a polycrystalline specimen of $PbNb_2O_6$ containing 2% by weight of $ZrTiO_4$. A smaller tetragonal structure cell than that indicated in Fig. 1 can be chosen, containing 5 molecules and with dimensions $a_0 = 12{\cdot}46$, $c_0 = 3{\cdot}907$ Å.

X-ray powder photographs indicate that there is a very close resemblance between the paraelectric structure of $PbNb_2O_6$ and that of certain tetragonal alkali tungsten bronzes, such as $K_{0{\cdot}57}WO_3$ and $Na_{0{\cdot}28}WO_3$ (Magnéli & Blomberg, 1951). Both tetragonal $PbNb_2O_6$ and these potassium and sodium bronzes may be classed with the 'tunnel-type' compounds discussed by Shlenck (1951) and Wadsley (1955). Fig. 2 shows a projection of the tetragonal bronze structure and illustrates how the K^+ or Pb^{2+} ions may be sited in 'tunnels' or 'cages' formed respectively by 5- or 4-membered rings of WO_6 or NbO_6 octahedra. The 'cages' comprise residual fractions of an ABO_3 perovskite structure, and enclose spaces normally occupied by the A ions. The 'tunnels' are simply channels running through the structure in the [001] direction. This arrangement provides 10- and 8-fold oxygen co-ordination in the 'tunnel' and 'cage' sites respectively.

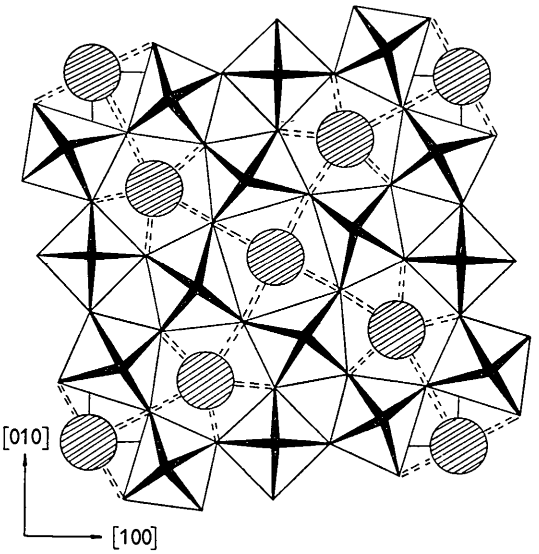

Fig. 2. Structure of paraelectric $PbNb_2O_6$, or $K_{0.57}WO_3$ (after Wadsley, 1955). Pb^{2+} or K^+ ions are shown as circles ($z = 0$) located in 'tunnels' or 'cages' formed by NbO_6 or WO_6 octahedra ($z = \pm\frac{1}{2}$).

From the projection in Fig. 2 it is seen that there are six possible sites for A-type ions in the unit cell. Of these, four are 10- co-ordinated 'tunnel' sites and the remaining two are 8- co-ordinated 'cage' sites. In $PbNb_2O_6$ only five of the total six are filled with Pb^{2+} ions, but at present, in the absence of high-temperature single-crystal data, no firm conclusions can be drawn as to how the Pb^{2+}-type vacancies are ordered. Also it is not known whether or not the high-temperature tetragonal structure retains the doubled c_0 dimension typical of the ferroelectric orthorhombic form.

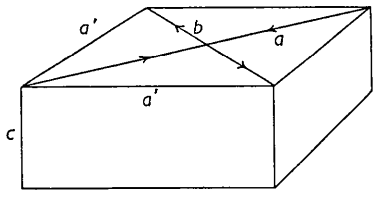

Fig. 3. Unit-cell axes in $PbNb_2O_6$. a' axes of tetragonal paraelectric structure. $a\,b$ axes of orthorhombic ferroelectric structure.

The structure change produced by the appearance of a polar moment on cooling below the Curie temperature occurs through a [110]-type deformation and, referred to the tetragonal bronze unit cell, the ferroelectric structure possesses monoclinic symmetry. Fig. 3 shows the relation of the orthorhombic a and b axes to the shorter a' axes of the high-temperature form.

4. Dielectric properties of ferroelectric $PbNb_2O_6$

The permittivity-temperature curve of ceramic orthorhombic $PbNb_2O_6$ shows a normal ferroelectric-type relation with a peak permittivity of about 7000 at 560 °C. As previously reported (Francombe, 1956) single crystals show marked anisotropy. The permittivity along each crystallographic axis was found by measuring the capacitance of a crystal provided with electrodes on faces perpendicular to the chosen axis, as identified by X-ray and optical examination. The capacitance measurements were made at 159 or 500 kc.sec.$^{-1}$ using an inductance ratio arm bridge. The results, given in Fig. 4, show that along the c axis the permittivity is almost independent of temperature, but that along either of the other perpendicular axes it shows a sharp peak at 560 °C. with a maximum permittivity of about 24000. At lower temperatures ε_a and ε_b are both lower than ε_c. The difference between ε_a and ε_b is small and approaches the limit of accuracy of the permittivity values. Because of the difficulty of measuring the dimensions of the rather irregularly shaped crystals the absolute values of permittivity may be in error by as much as ±20%.

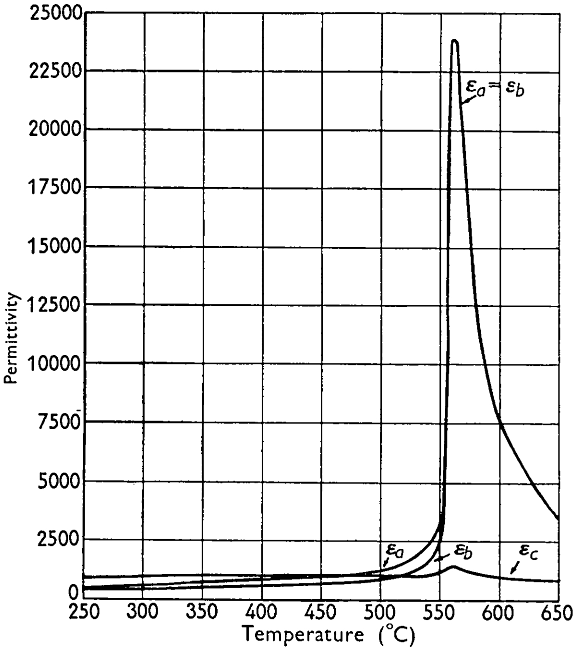

Fig. 4. Permittivity of $PbNb_2O_6$.

However, the permittivity along the a and b axes, of crystals with only a small amount of twinning, appeared to be identical at and above the Curie point, with ε_a somewhat greater than ε_b at lower temperatures. Taken in conjunction with the crystallographic data of the previous section these results indicate a ferroelectric transition at 560 °C. with the anomalous polarization confined to the a–b plane. By analogy with $BaTiO_3$, in which the polar axis in the ferroelectric state is elongated and has a lower permittivity, the b axis is probably the polar axis.

Hysteresis loops at 50 $c.sec.^{-1}$ and 30 $kV.cm.^{-1}$ for both crystals and ceramics show only very slight non-linearity with no indication of saturation, and a very low remanent polarization. Poling in a unidirectional field of 20 $kV.cm.^{-1}$ at 200 °C. for an hour produced remanent polarization in a- and b- crystals and in ceramics, as indicated by pyroelectric and piezoelectric changes of polarization with temperature and pressure, respectively. These measurements show that the field required for the alignment of the polar axis along the field direction is very high in both crystals and ceramics. Some of the reasons for this become apparent on studying the domain patterns in single crystals.

5. Optical and domain properties of $PbNb_2O_6$ crystals

In plate-like crystals of orthorhombic $PbNb_2O_6$ obtained by growth from the melt the c axis was perpendicular to the plate surface. Several of these, ranging in size up to about 2 mm. × 1 mm. × 0·3 mm. were of good quality and showed sharp and nearly perfect extinction between crossed polaroids.

The refractive indices have been determined by the embedding method using sulphur–selenium melts (Larsen & Berman, 1934). The medium is deep red in colour and the light transmitted approximates to lithium light. By embedding in Se–6% S($n_{\mathrm{Li}} = 2{\cdot}60$), Se–12% S($n_{\mathrm{Li}} = 2{\cdot}50$), Se–16% S($n_{\mathrm{Li}} = 2{\cdot}45$) and Se–20% S($n_{\mathrm{Li}} = 2{\cdot}40$), the refractive indices were found, to within $\pm 0{\cdot}01$, as $\alpha_{\mathrm{Li}} = 2{\cdot}40$ parallel to a, $\beta_{\mathrm{Li}} = 2{\cdot}43$ parallel to b and $\gamma_{\mathrm{Li}} = 2{\cdot}60$ parallel to c.

Viewed along the c axis, and in the extinction position, the crystals show (Plate 9(a)) a network of narrow orthogonal bands, at approximately 45° to the a and b axes, which remain bright. The orientation of these bands is that expected for 90° domains, bounded by $\{110\}$ twin planes. Their appearance under normal lighting is shown in Plate 9(b). Fig. 5 shows that the continuity of normal electrical polarization is maintained when the boundaries make an angle of 44° 35′ with the b axis. Similar considerations show that a 180° boundary, between domains with antiparallel polarization vectors, must be along the b axis.

The interpretation of the bands as 90° domains is confirmed by the appearance of a multi-domain c-plate embedded in a medium which matches one of the refractive indices α or β. For one orientation of the plane of polarization of incident light the crystal is invisible except for its domains, its outline showing up only where a 90° domain goes right to the edge. With the perpendicular orientation, the outline of the crystal can be seen except at the positions of 90° domains. Large 90° domains, or twins, are rare except in larger and less perfect crystals.

Plate 9(f) and (g) illustrates a change in the appearance of the domains as the refractive indices α and β are interchanged by rotation of the plane of polarization of the incident light, with no embedding medium. In (f) the plane of polarization is such that the crystal exhibits its refractive index β, except for the domains which have $n = \alpha$. The domains show up dark against a light ground. In (g) the polarizer has been rotated through 90° and the domains are light with shadowy edges against a light ground. This effect can be explained by total internal reflexion of oblique light, or a cone of light, as it passes through the crystal, at the interfaces between the domains and the bulk crystal, as illustrated diagrammatically in Fig. 6. The incident light is scattered, either away from or into the domain, dependent on the value of the refractive index of the domain compared with that of the surrounding crystal.

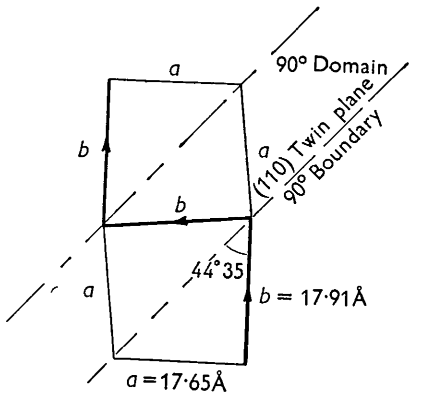

Fig. 5. Geometry of 90° boundaries in $PbNb_2O_6$.

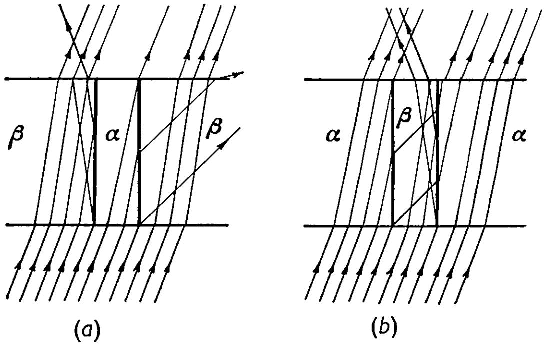

Fig. 6. Transmission of oblique light incident on a crystal containing a narrow 90° domain. (a) Refractive index of crystal = β, of domain = α. (b) Refractive index of crystal = α, of domain = β.

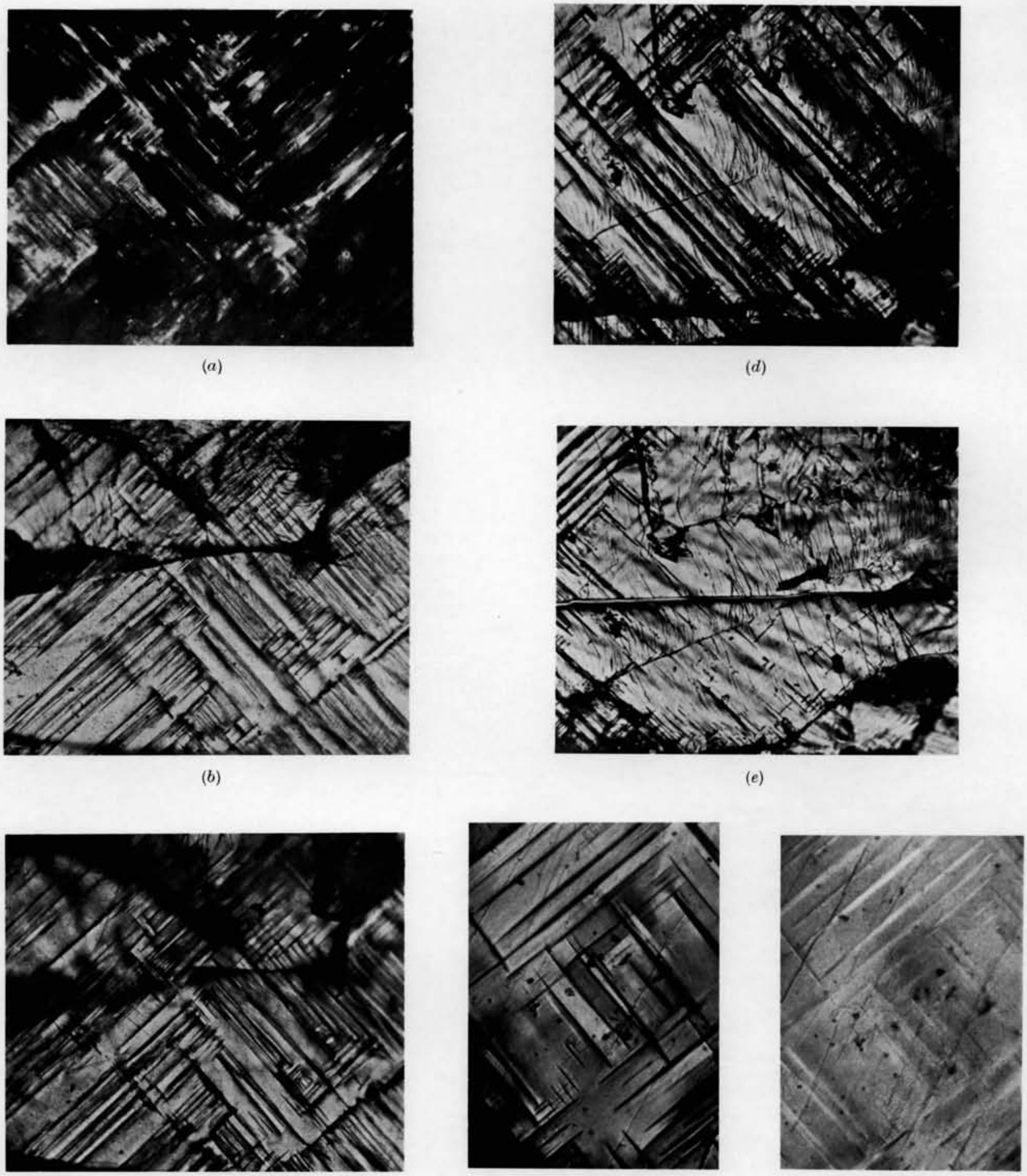

(a) (d) (b) (e) (c) (f) (g)

Ferroelectric domains in $PbNb_2O_6$. (*a*) $PbNb_2O_6$ crystal at extinction between crossed polaroids (× 100). (*b*) Same crystal as (*a*) in plane polarized light (× 100). (*c*) Reverse side at crystal shown in (*b*). Photograph reversed in printing to facilitate comparison (× 100). (*d*) $PbNb_2O_6$ crystal showing 90° domain structure (× 150). (*e*) Same crystal as (*d*) after heat treatment (× 150). (*f*) $PbNb_2O_6$ crystal showing details of 90° domain structure, plane of polarization of incident light parallel to *a*-axis of crystal and *b*-axis of domains (× 500). (*g*) Same crystal as (*f*), plane of polarization of light rotated through 90° (× 500).

In order to avoid very large shear strains the b axis in any part of the crystal must maintain its orientation in each successive atomic layer normal to the c direction. Hence the same domain pattern should be seen on the top and bottom of any crystal. Plate 9(*c*) shows the other side of the same crystal as in (*b*), but has been reversed in printing to facilitate comparison of the domain patterns. It will be seen that the main features of the patterns are the same, but that there are differences of detail which suggest that some domains taper and disappear within the thickness of the crystals. There is less perfect correspondence between the domain patterns on either side of crystals thicker than about 1 mm.

Observations at elevated temperatures have been made by heating the crystal, on the microscope stage, in a small loop of platinum wire. Above 560 °C. the domain pattern disappears, confirming that it is directly associated with the ferroelectric state of the crystal. On cooling again to below the Curie point, domains reappear but the pattern is usually very much simpler than it was before. Photographs of a crystal, at room temperature, before and after such heat treatment are shown in Plate 9(*d*) and (*e*). Most of the original domains have been removed by the heat treatment and some new ones have appeared together with a crack extending across the crystal.

The domain geometry illustrated in Fig. 5 shows that for an unstrained crystal the boundaries on either side of the domain should be parallel. The presence of wedge-shaped domains, as in Plate 9(*f*), indicates that shear strain and bound electrostatic charge must be distributed along the domain walls. However, at the temperature at which the domains are formed, conductivity is quite sufficient to allow the migration of free charge to balance the bound charge and thus reduce the electrostatic energy. The 90° domains probably form in such a way as to relieve the internal strain associated with irregularities and defects in the crystal lattice, and thus to minimize the strain energy. At room temperature, where the mobility of lattice defects and of free charge are low, the boundaries will be strongly held at their equilibrium positions.

Untwinned regions of the crystal probably contain domains with antiparallel polarization vectors separated by 180° boundaries. These boundaries should lie along the b axis and thus at 44° 35′ to the 90° boundaries but, as in the case of $BaTiO_3$, they will not normally be visible. There is no strain or charge discontinuity associated with such a 180° boundary and, under the influence of an external electric field, favourably oriented domains might be expected to grow quite freely, either by sideways movement of 180° boundaries or by nucleation and forward growth as a wedge. However, where a 180° boundary meets or crosses a 90° boundary it is obviously impeded, and 180° boundaries which intersect 90° domains are probably held strongly in equilibrium positions.

The conclusion is that a complex network of 90° domains, such as is generally observed, indicates a very stable arrangement which requires high energy to re-arrange it. Attempts to produce changes in the domain pattern by the application of an electric field along the a or b axis failed to show any detectable movement of the 90° boundaries, in fields up to 5 kV.cm.$^{-1}$ and at temperatures up to 300 °C.

6. The system $PbO.x(Nb_2O_5)$, where $1 \leq x \leq 3$

The similarity between the high-temperature structure of $PbNb_2O_6$ and the structure of the tetragonal tungsten bronzes, such as $K_{0·57}WO_3$ and $Na_{0·28}WO_3$, suggested that analogous 'tunnel-type' structures might well be found for niobates containing a higher proportion of Pb^{2+} vacancies. X-ray studies were thus made of $PbO.x(Nb_2O_5)$ compounds with nominal x values of 1, 1·15, 1·25, 1·4, 1·5, 2·0 and 3·0. When possible single crystals were examined optically and, for two compositions, $x = 1·5$ and 2·0, electrical measurements were made.

6·1. *Structure*

The compositions examined were all found to possess very similar crystal structures. The progressive removal of lead from the $PbNb_2O_6$ lattice reduces the orthorhombic distortion and, for the composition $PbO.3(Nb_2O_5)$, fully tetragonal bronze-type symmetry is produced. The variation of the orthorhombic unit-cell dimensions with composition, shown by the X-ray powder studies of sintered specimens, is depicted in Fig. 7. As x is increased from 1·0 to 1·5 there is a marked, discontinuous change in the lattice parameters, and in this composition range it was found very difficult to obtain single-phase structures with good homogeneity. There is a strong tendency, especially at $x = 1·25$, for disproportionation into two

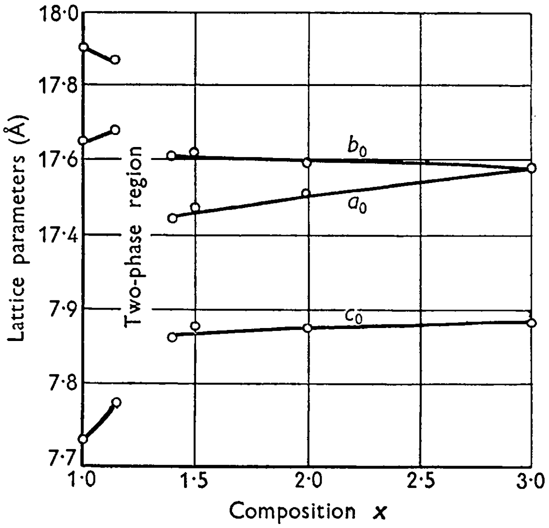

Fig. 7. Lattice parameters of compositions $PbO.x(Nb_2O_5)$.

phases to occur. This effect becomes more pronounced with increased firing periods, and for samples fired for 2 hours at 1280 °C. two homogeneous phases, with unit-cell dimensions similar respectively to those for compositions $x = 1{\cdot}0$ and $1{\cdot}5$, were obtained.

Summarising these results it is possible to distinguish between two different structures in the composition range considered here. Thus at $x = 1$ we have the heavily distorted orthorhombic structure of ferroelectric $PbNb_2O_6$, which appears to permit of only a very small deviation from stoichiometry, while for $1{\cdot}5 \leq x \leq 3{\cdot}0$ a pseudo-tetragonal (truly orthorhombic) bronze-type structure, analogous to $Na_{0{\cdot}28}WO_3$, is produced, displaying wide departures from stoichiometry.

The most striking difference between these structures lies in the sudden expansion of the c_0 dimension as x is increased from 1·0 to 1·5. This expansion is probably associated with a straightening of the Nb–O–Nb bonds leading to the formation of linear chains of NbO_6 octahedra, typical of cubic perovskite niobates. In $NaNbO_3$ this straightening is characterized by a spacing of 3·942 Å between Nb ions in the chain (Francombe & Lewis, 1957). Single-crystal rotation photographs taken about the c axis for the lead niobates show that the weak 'extra' layer lines indicating a doubled c_0 dimension gradually disappear as x increases, and for $x > 2$ the true c_0 spacing is therefore half that shown in Fig. 7. As x approaches 3 the separation of Nb ions in the chain is about $7{\cdot}88/2 = 3{\cdot}94$ Å, and is thus very close to that for cubic $NaNbO_3$.

6·2. *Optical and electrical studies*

Examination of single crystals with nominal compositions $PbO.1{\cdot}5(Nb_2O_5)$ and $PbO.2{\cdot}0(Nb_2O_5)$ by microscopic methods showed both to comprise green, tablet-shaped or columnar crystals. In polarized light the crystals were found to be optically biaxial with straight extinction. X-ray single-crystal studies showed that the orthorhombic c direction, in each case, lay along the long edge of the tablet or column. The principal cleavage planes were of the (100) and (010) type.

Crystals with the nominal composition $PbO.1{\cdot}25(Nb_2O_5)$ were found to consist of greenish-yellow crystalline lumps with very irregular shapes. Both the colour and the absence of regular plate-like or columnar shape are consistent with the mixture of two phases found from the X-ray powder data.

Dielectric measurements were carried out at different temperatures on ceramic specimens possessing the nominal compositions $x = 1{\cdot}5$ and $2{\cdot}0$. No permittivity anomalies were observed for either preparation, and it was concluded that these compositions were not ferroelectric. These observations were confirmed for the second compound using a tablet-shaped single crystal of the same approximate composition.

7. The system $PbNb_2O_6$-$PbTa_2O_6$

Ceramic specimens of $PbTa_2O_6$ and of solid solutions $PbNb_2O_6$–$PbTa_2O_6$ were fired in air, as pressed discs, in the range 1300 °C. to 1400 °C.

X-ray powder studies of $PbTa_2O_6$ show that it is structurally very similar to $PbNb_2O_6$, except that its symmetry is fully tetragonal and like that of tungsten-bronze. The unit-cell dimensions are $a_0 = 12{\cdot}49$, $c_0 = 3{\cdot}875$ Å. In dealing with $PbNb_2O_6$-type solid solutions, it is convenient to refer to the orthorhombic axes and to assume a doubled c_0 parameter. The variation of lattice parameters, Fig. 8, for the system $PbNb_2O_6$–$PbTa_2O_6$ shows a complete range of solid solution. As the concentration of tantalum increases the orthorhombic b_0 parameter progressively decreases,

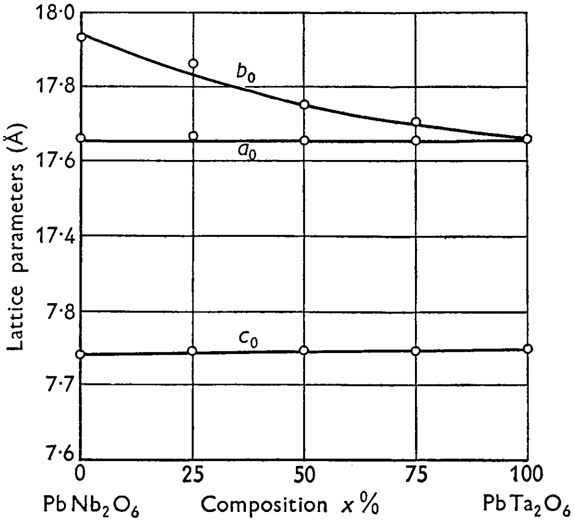

Fig. 8. Lattice parameters of compositions $(1-x)PbNb_2O_6.xPbTa_2O_6$.

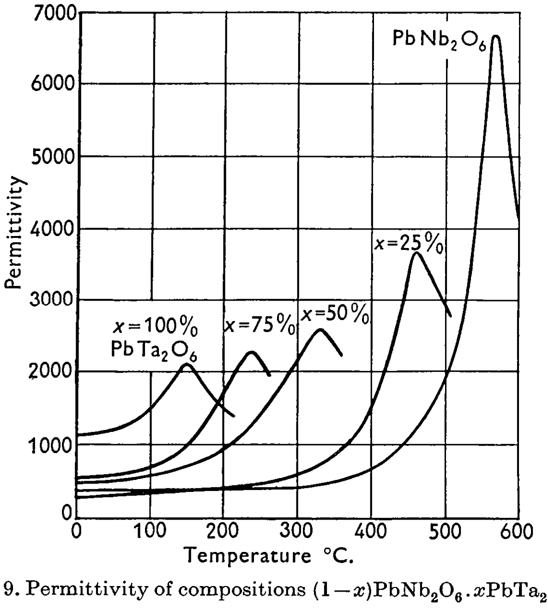

Fig. 9. Permittivity of compositions $(1-x)PbNb_2O_6.xPbTa_2O_6$.

while the a_0 and c_0 parameters remain substantially unchanged over the entire solid-solution range.

Dielectric measurements, Fig. 9, show a corresponding decrease of Curie temperature, down to 150 °C. for $PbTa_2O_6$. The sharpness and height of the permittivity peaks is, however, reduced compared with $PbNb_2O_6$, indicating a progressive weakening of the ferroelectric character.

8. Discussion

The experimental data presented here for single crystals show that orthorhombic $PbNb_2O_6$ represents a new type of 'two-dimensional' ferroelectric structure. In other structures composed of networks of oxygen octahedra and possessing pseudo-cubic symmetry, for example the perovskite-like $BaTiO_3$ and $KNbO_3$, and the pyrochlore-like $Cd_2Nb_2O_7$, there are three possible axial directions (the cube edges) along which spontaneous polarization can occur. The crystal symmetry of $PbNb_2O_6$, however, permits only of two such directions, which are identified with the [100] or [010] axes of the orthorhombic structure cell.

On cooling through the Curie point at 560 °C. the change of structure from tetragonal to orthorhombic is associated with very large anisotropic strain effects. At room temperature, the ferroelectric strain b_0/a_0 is 1·016, compared with $c_0/a_0 = 1{\cdot}01$ for tetragonal $BaTiO_3$. Such high spontaneous strain effects are also found in the perovskite-type ferroelectrics $PbTiO_3$ and $PbZrO_3$, and Megaw (1954) has suggested that they arise partly from the tendency of the Pb ion to form covalent bonds of the type found in PbO. In the monoxide structure the Pb ion is situated at the apex of a flat, square-based pyramid with oxygen ions at the four corners (Wells, 1950).

A similar explanation may be advanced to account for the somewhat anomalous behaviour of the orthorhombic cell dimensions on passing through the Curie temperature (Fig. 1). If, as has been suggested, the b axis of the unit cell becomes the direction of spontaneous ferroelectric strain, then by analogy with other ferroelectric structures, we should expect an expansion along this axis to be accompanied by relative contractions along the a and c axes. In fact expansions are observed along both a and b axes, associated with a sharp contraction along the c axis. This may be explained if the observed deformations originate from two causes operating simultaneously. One of these would be the sudden appearance of a spontaneous ferroelectric strain which tends to produce a b-axis expansion, and hence relative a- and c-type contractions. The second would arise from a sudden increase in the covalent character of the Pb–O bonds, which produces a sharp c-axis contraction accompanied by relative expansions of both a_0 and b_0 dimensions referred to the high-temperature tetragonal a_0 parameter.

Our present knowledge of the orthorhombic $PbNb_2O_6$ structure and its relation to the tetragonal bronze structure is still greatly lacking in detail, and no information is yet available regarding the positions of the Pb or Nb ions relative to the undisplaced sites in the tetragonal lattice. If covalent bonds of the type suggested for Pb ions were formed, the ions most likely to be involved would appear to be those in the 'cage' sites (Fig. 2). Covalent bonding would thus tend to draw the Pb ion towards the four oxygen ions either above or below it, as shown in Fig. 10, producing a contraction in the c direction. The Pb–O bonds to the remaining oxygen ions would presumably be more ionic in character and should give rise to easy (001)-type cleavage. A strong cleavage of this type is in fact observed with pure $PbNb_2O_6$ crystals. Moreover, removal of lead from the lattice, giving compositions such as $PbO.x(Nb_2O_5)$ with x values of 1·5 and 2·0, results in the almost complete disappearance of the c-axis contraction, and in a sharp change in the principal cleavage from (001) to (100) and (010) planes.

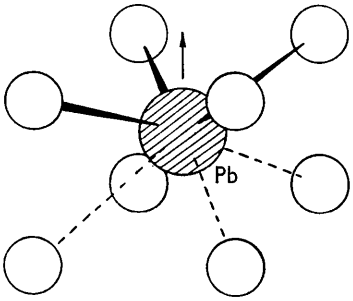

Fig. 10. Suggested arrangement of pyramidal bonds for Pb ion in 'cage' site of $PbNb_2O_6$ structure.

The single-crystal X-ray data for $PbNb_2O_6$ are consistent with the view that the Nb ions are puckered relative to the (001) planes, as has been suggested for the W ions in the compound $Na_{0{\cdot}28}WO_3$ (Magnéli & Blomberg, 1951). Also, since the spontaneous polarization effect is along the b axis of the orthorhombic structure cell, it is probable that parallel displacements of Nb ions occur in this direction. The puckering probably arises from tilting of the NbO_6 octahedra relative to the c axis, as has been suggested by Megaw (1954) for certain pseudo-cubic perovskites such as $CaTiO_3$. This effect alone, however, would not explain the ferroelectric properties, which appear to involve additional parallel Nb displacements referred to the oxygen framework.

The fact that progressive replacement of Nb by Ta in the $PbNb_2O_6$–$PbTa_2O_6$ solid solutions reduces the b_0 orthorhombic parameter, while the a_0 and c_0 parameters show no significant change, is in keeping with a reduction of ferroelectric strain in the b direction and with the observed fall in the Curie temperature. Covalent Pb–O bond formation should affect both the $PbNb_2O_6$ and $PbTa_2O_6$ structures to about the same extent, and may well account for the similarity in the c_0 parameter.

The Pb ion apparently plays an important role in maintaining strong linkages between NbO_6 octahedra in the (001) planes. Removal of more than a small amount of Pb from the lattice seems to result in a breakdown of these linkages, and of the co-operative ionic displacements associated with ferroelectricity.

References

Francombe, M. H. (1956). *Acta Cryst.* **9**, 683.

Francombe, M. H. & Lewis, B. (1957). *J. Electronics*, **2**, 387.

Goodman, G. (1953). *J. Amer. Ceram. Soc.* **36**, 368.

Jona, F., Shirane, G. & Pepinsky, R. (1955). *Phys. Rev.* **98**, 903.

Larsen, E. S. & Berman, H. (1934). *Microscopic Determination of the Nonopaque Minerals*, 2nd ed., p. 848. Washington: U.S. Geol. Survey Bulletin.

Magnéli, A. & Blomberg, B. (1951). *Acta Chem. Scand.* **5**, 372.

Matthias, B. T. (1951). *Science*, **113**, 591.

Matthias, B. T. & Remeika, J. P. (1949). *Phys. Rev.* **76**, 1886.

Megaw, H. D. (1954). *Acta Cryst.* **7**, 187.

Roth, R. S. (1957). *Acta Cryst.* **10**, 437.

Shirane, G., Danner, H., Pavlovic, A. & Pepinsky, R. (1954). *Phys. Rev.* **93**, 672.

Shlenck, W. (1951). *Fortschr. Chem. Forsch.* **2**, 92.

Wadsley, A. D. (1955). *Reviews of Pure and Applied Chem.* **5**, 165.

Wells, A. F. (1950). *Structural Inorganic Chemistry*, 2nd ed., p. 636. Oxford: Clarendon Press.

Acta Cryst. (1958). **11**, 703

The Crystal Structure of Nolanite

By A. W. Hanson

Division of Pure Physics, National Research Council, Ottawa, Canada

(*Received* 10 *March* 1958)

Nolanite is hexagonal, probably $P6_3mc$, with $a = 5{\cdot}85$, $c = 9{\cdot}29$ Å, and formula approximately $Fe^{+2}_{2\cdot5}V^{+3}_{1\cdot5}V^{+4}_{6}O_{16}$. The structure, which was refined by c- and a-axis projections, consists of a close-packed hexagonal (*ABAC*) framework of 16 oxygen anions, with metal ions in some of the interstices. The tetravalent vanadium ions occupy a 6-fold position of octahedral coordination, while the iron and trivalent vanadium ions are distributed among two 2-fold positions (on the 3-fold axes), one of octahedral and one of tetrahedral coordination. Results obtained with different radiations suggest that trivalent vanadium has a strong, but not exclusive, preference for tetrahedral coordination.

Introduction

The recently-named iron–vanadium mineral Nolanite has been discussed by Barnes & Qurashi (1952) and by Robinson, Evans, Schaller & Fahey (1957). Their crystallographic conclusions may be summarized as follows:

Nolanite is hexagonal, $P\bar{6}2c$, $P6_3mc$, or $P6_3/mmc$

$$a = 5{\cdot}854 \pm 0{\cdot}005,\quad c = 9{\cdot}295 \pm 0{\cdot}010 \text{ Å}\,.$$

The structure suggested by the unit cell is a framework of 16 close-packed oxygen anions, with cations in some of the interstices.

Two chemical analyses are quoted, one for a reasonably large sample of impure massive material, and the other for 25 mg. of hand-picked crystalline material. Assuming 16 anions per unit cell, the chemical formulae suggested by these analyses are, respectively

$$Fe^{+2}_{2\cdot8}V^{+3}_{1\cdot5}V^{+4}_{5\cdot5}O_{16\cdot0} \quad \text{(analysis 1)}$$

and

$$Fe^{+2}_{2\cdot5}V^{+3}_{1\cdot7}V^{+4}_{5\cdot5}O_{16\cdot0} \quad \text{(analysis 3)}\,.$$

Because of recognized uncertainties in the analyses, no definite chemical formula was given.

It is suggested on crystal chemical grounds that there are 10 cations in the unit cell. Moreover, it is expected that iron may substitute for vanadium on one or more crystallographic sites, so that the Fe:V and V^{3+}:V^{4+} ratios need not be rational.

Assumptions for the present paper

In what follows, the chemical formula is assumed, for convenience, to be

$$(Fe, V)_4V_6O_{16}$$

where (Fe, V) is a composite ion such that $(Fe,V)_4 = 2{\cdot}5\ Fe^{2+} + 1{\cdot}5\ V^{3+}$ and V is tetravalent vanadium. This formula was obtained, somewhat arbitrarily, by averaging the two given in the preceding section, and rounding out the quantities to integral values. It will be shown that the assumption of this formula leads to a plausible structure which is consistent with the X-ray data. Nevertheless, it must be emphasized that the